

**Tikrit University**  
**College of Science**  
**Physics department**



**Submitted by the student:**

**Ms.c Muzahim Aziz Abdullah**

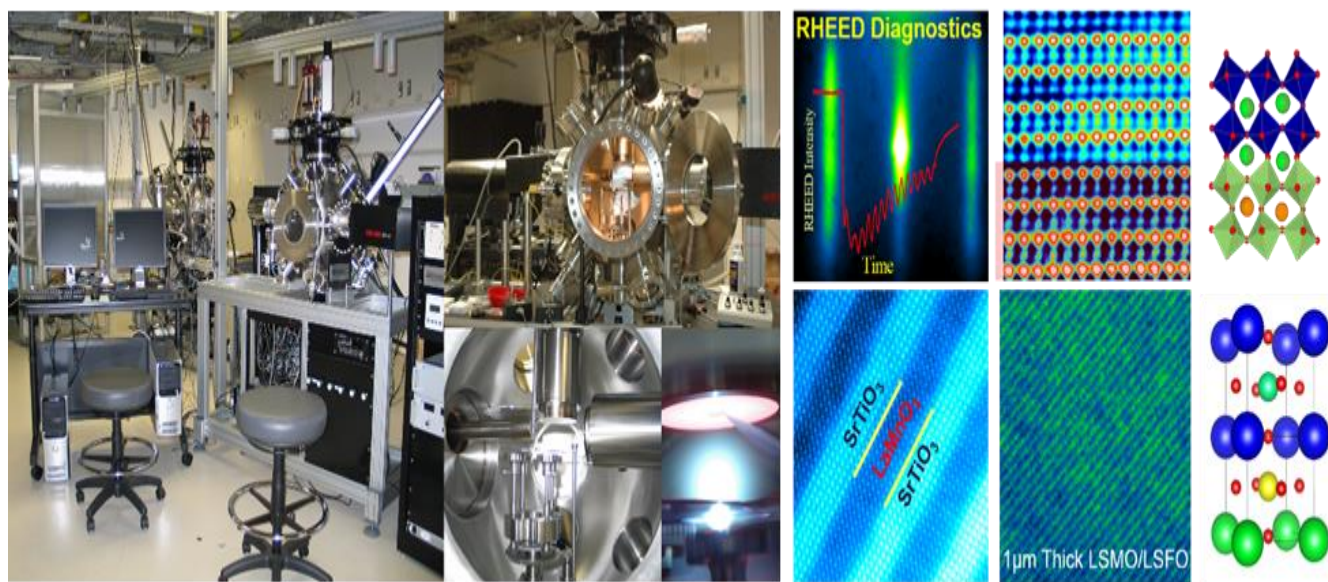
**THIN-FILM DEPOSITION BY LASER TECHNOLOGY**

**Supervisor :**

**Prof.Dr.Najat Ahmed Dahham**

**2019/2020**

# PULSED LASER DEPOSITION OF THIN FILMS



Pulsed laser deposition typically uses a pulsed nanosecond laser beam to vaporize pellets of target material in a low pressure, typically oxygen-containing, environment. Under these conditions, a nearly stoichiometric “plume” of that material is transported to a heated substrate where the material nucleates to create well-controlled thin films, or layered structures of multiple films, with nanometer-scale precision<sup>(1)</sup>. This type of synthesis is performed to explore the effects of interfaces, confinement, and coupling between layers. The type of materials are typically complex metal-oxides that contain several atomic elements.

## SCIENCE OVERVIEW

The CNMS pulsed laser deposition facilities are designed for thin film deposition in oxygen, argon, and a mixed ambient, if required. The incident excimer laser beam is delivered to one of 4 targets using a projection beamline, meaning spot size is easily adjusted and laser fluence at the target is fairly uniform. The benefits of this type of beam delivery are twofold: first, growth rates can be easily tuned to between low rates for superlattices or higher rates for more conventional films, and second, growth

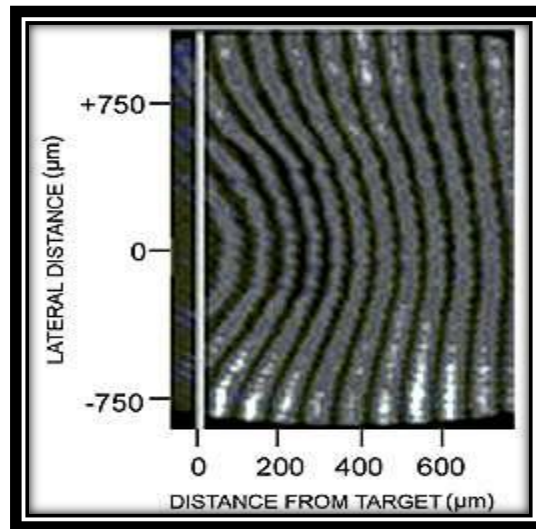
parameters are easily reproduced on future user visits as well as being easily translated to other PLD labs<sup>(2)</sup>. For materials with sufficient structural perfection to also exhibit a layer-by-layer growth mode, film thickness evolution can be monitored using high pressure reflection high energy electron diffraction (RHEED).

## **APPLICATIONS**

The CNMS PLD facilities are used to synthesize a range of thin film materials to explore diverse phenomena ranging from spin ices and proton conduction to magnetic ordering and morphologically-induced phase composition.

The technique of PLD was found to have significant benefits over other film deposition methods, including:

1. The capability for stoichiometric transfer of material from target to substrate, i.e. the exact chemical composition of a complex material such as YBCO, can be reproduced in the deposited film.
2. Relatively high deposition rates, typically  $\sim 100 \text{ s } \text{\AA}/\text{min}$ , can be achieved at moderate laser fluences, with film thickness controlled in real time by simply turning the laser on and off.
3. The fact that a laser is used as an external energy source results in an extremely clean process without filaments. Thus deposition can occur in both inert and reactive background gases.
4. The use of a carousel, housing a number of target materials, enables multilayer films to be deposited without the need to break vacuum when changing between materials<sup>(3)</sup>.

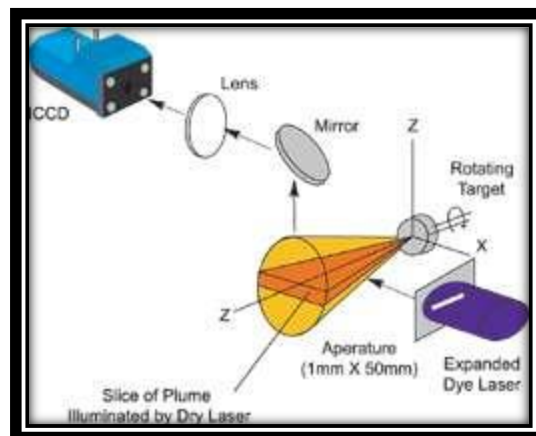


Interferogram of a Magnesium plasma plume expanding into vacuum taken 46 ns after the ablation pulse struck the target surface. Laser fluence  $(2.0 \pm 0.2)$  J/cm<sup>2</sup> on target, 2 ns ICCD gate width. Image courtesy of Physics Department, Queen's University, Belfast.

In spite of these significant advantages, industrial uptake of PLD has been slow and to date most applications have been confined to the research environment. There are basically three main reasons for this:

1. The plasma plume created during the laser ablation process is highly forward directed, therefore the thickness of material collected on a substrate is highly non-uniform and the composition can vary across the film. The area of deposited material is also quite small, typically  $\sim 1 \text{ cm}^2$ , in comparison to that required for many industrial applications which require area coverage of  $\sim (7.5 \times 7.5) \text{ cm}$ .
2. The ablated material contains macroscopic globules of molten material, up to  $\sim 10 \mu\text{m}$  diameter. The arrival of these particulates at the substrate is obviously detrimental to the properties of the film being deposited.
3. The fundamental processes, occurring within the laser-produced plasmas, are not fully understood; thus deposition of novel materials usually involves a period of empirical optimization of deposition parameters<sup>(4)</sup>.

To a large extent the first two problems have been solved. Films of uniform thickness and composition can be produced by rastering the laser spot across the target surface and / or moving the substrate during deposition. Line-focus laser spots have also been used to obtain large area coverage. The particulate material was initially removed from the plume using a mechanical velocity filter, although recently more elaborate techniques, involving collisions between two plasma plumes or off-axis deposition, have been used to successfully grow particulate-free films. The third problem will be resolved by the development of computer simulations to describe PLD, and will further our understanding of the fundamental physics and chemistry involved in the deposition process. However, a large amount of experimental data, obtained under accurately controlled and defined conditions, is required to assist the verification of such models<sup>(5)</sup>.

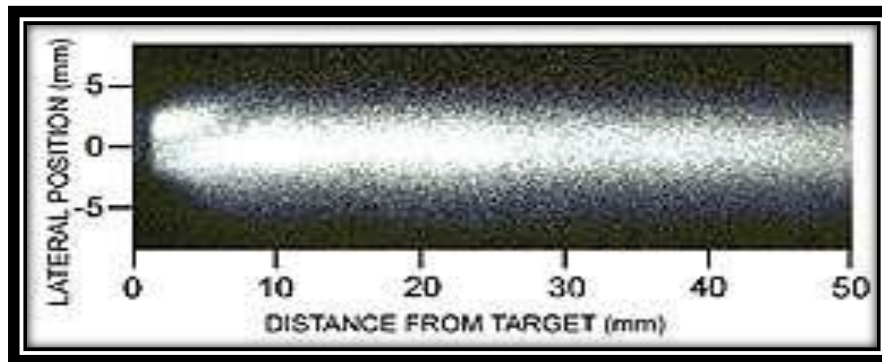


Typical system configuration for LIF data acquisition

The PLD process can be crudely split into two sections, i.e. the plasma creation and expansion, followed by film growth at the substrate. In the current article only data relating to the initial stage will be presented. The temporal evolution of densities, temperatures and velocities within laser-produced plasmas can only be determined using fast diagnostics ( $\sim$ ns time-scales), due to the high luminosity and transient nature of the plumes.

A variety of techniques, including interferometry, optical spectroscopy and Laser-Induced Fluorescence (LIF), are used to

investigate different stages of the plasma creation and expansion. At short delay times after the ablation pulse ( $<100\text{ns}$ ) Mach-Zehnder interferometry has been used to study the free electron component within the plume expanding into vacuum. The time-varying electron density was calculated from a series of interferograms of the plume, captured using an Andor ICCD camera with a  $2\text{ns}$  gate width. A typical image is shown in the on the left<sup>(6)</sup>.

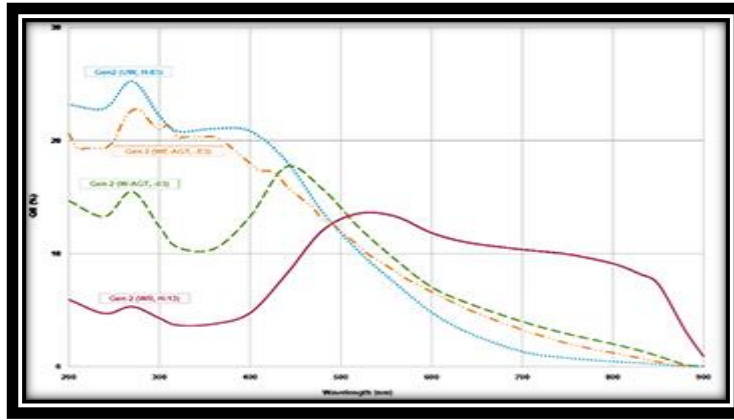


LIF image of ground state, singly ionized Titanium species expanding along the target normal into vacuum. The image was recorded  $3\mu\text{s}$  after the ablation pulse struck the target surface and at a laser fluence of  $(5.1 \pm 0.2) \text{ JCM}^{-2}$ . Image courtesy of Physics Department, Queen's University, Belfast.

The plume emits high intensity broadband emission during the initial stages of the expansion, which could easily saturate the detector. However, the short gate width of the ICCD blocks out the majority of this continuum emission, enabling the interferogram to be "extracted" from the larger background signal. These "snapshots" show measurable electron densities extending out to  $\leq 1\text{mm}$  from target at these delays with peak densities  $>10^{17}\text{cm}^{-3}$ , calculated using an Abel inversion technique. At longer delays (and under similar conditions) LIF was used to map the neutral and ionic components within slices of the plume. A typical experimental configuration used to obtain LIF measurements is illustrated on the right.

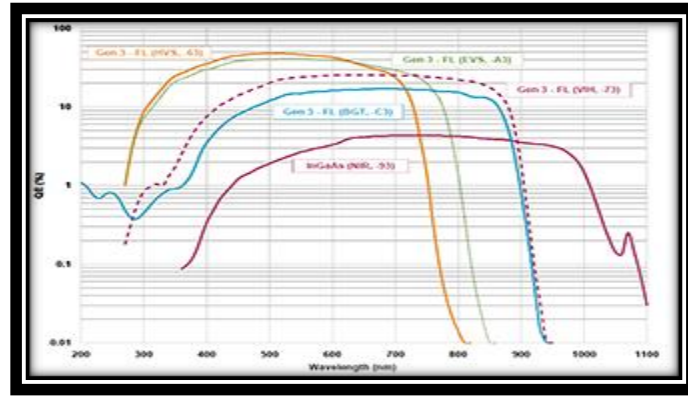
The picture on the left shows a LIF image of ground state Ti II ions within a plume, recorded with a  $5\text{ns}$  ICCD gate width.





Gen 2 photocathode QE curves relevant to Pulsed Laser Deposition

Once again the short gate width is required to extract the relatively weak LIF signal from the more intense plasma self-emission. The signal was observed to extend beyond 50mm at 3 $\mu$ s delay, with peak densities  $\sim 10^{10}$ cm $^{-3}$  (obtained using a combination of LIF and absorption spectroscopy data). Data from these diagnostics were used to construct an overall picture of the plume expansion for comparison with models of the laser ablation process<sup>(7)</sup>. These two examples show both the species density and spatial extent of the plume varying over several orders of magnitude during a timescale of less than a few microseconds, illustrating the flexibility required from both the diagnostics and detectors used in such experimental investigations<sup>(8)</sup>. As our understanding of the plasma processes increases, these investigations and computer models may be applied to more complex systems than those considered in the present case and will include the deposition stage of the process. Eventually it is hoped that the computer simulations can be used for predictive purposes when novel materials are to be deposited using PLD. Fast ICCD's will continue to be the detector of choice for acquiring the data necessary to develop these computer models, with their role perhaps changing to in-situ monitors for process control, once PLD becomes commercially viable for industrial applications<sup>(9)</sup>.



Gen 3 photocathode QE curves relevant to Pulsed Laser Deposition

## SPECIFICATIONS

- Laser source: 248 nm excimer laser, 1 J/pulse, 1 Hz to 20 Hz repetition rate
- Number of targets: 4 with computer-controlled target sequencing
- Spot size at target: adjustable from sub millimeter to a few millimeters
- Fluence at target: adjustable from sub  $1 \text{ J/cm}^2$  up to  $4 \text{ J/cm}^2$
- Deposition rate: adjustable from sub angstroms per laser shot to almost 1 angstrom per laser shot
- In situ diagnostics: High pressure RHEED
- Base pressure:  $2 \times 10^{-7}$  torr
- Ambient: currently argon or oxygen, pressured controlled to multiple millitorrs up to 100s of millitorrs
- Heating: Radiant up to 800 C
- Substrate size: Based on laser plume dimensions, typically 5 mm x 5 mm or 10 mm x 10 mm for uniformity.
- Target-to-substrate: adjustable from 25 mm to 75 mm, but RHEED requires 40 mm.



## **References**

1. L. Bovo, C.M. Rouleau, D. Prabhakaran, and S.T. Bramwell, Phase transitions in few-monolayer spin ice films, *Nature Communications* **10**, 1219 (2019).
2. A. Herklotz, S.F. Rus, N. Balke-Wisinger, C.M. Rouleau, E.-J. Guo, A. Huon, K.C. Santosh, R. Roth, X. Yang, C. Vaswani, J. Wang, P. Orth, M.S. Scheurer, and T.Z. Ward, Designing Morphotropic Phase Composition in  $\text{BiFeO}_3$ , *Nano Letters* **19**, 1033 (2019).
3. K.A. Stoerzinger, X.R. Wang, J. Hwang, R.R. Rao, W.T. Hong, C.M. Rouleau, D. Lee, Y. Yu, E.J. Crumlin, and Y. Shao-Horn, Speciation and Electronic Structure of  $\text{La}^{1-x}\text{Sr}_x\text{CoO}_{3-\delta}$  During Oxygen Electrolysis, *Topics in Catalysis* **61**, 2161 (2018).
4. J. Ding, J. Balachandran, X. Sang, W. Guo, J.S. Anchell, G.M. Veith, C.A. Bridges, Y. Cheng, C.M. Rouleau, J.D. Poplawsky, N. Bassiri-Gharb, R.R. Unocic, and P. Ganesh, The Influence of Local Distortions on Proton Mobility in Acceptor Doped Perovskites, *Chemistry of Materials* **30**, 4919 (2018).
5. J. Ding, J. Balachandran, X. Sang, W. Guo, G.M. Veith, C.A. Bridges, C.M. Rouleau, J.D. Poplawsky, N. Bassiri-Gharb, P. Ganesh, and R.R. Unocic, Influence of Nonstoichiometry on Proton Conductivity in Thin-Film Yttrium-Doped Barium Zirconate, *ACS Applied Materials & Interfaces* **10**, 4816 (2018).

6. Y. Fujioka, J. Frantti, C. Rouleau, A. Puretzky, and H.M. Meyer, Vacancy filled nickel-cobalt-titanate thin films, *Physica Status Solidi (B)* **254**, 1600799 (2017).
7. K.A. Stoerzinger, R.R. Rao, X.R. Wang, W.T. Hong, C.M. Rouleau, and Y. Shao-Horn, The role of Ru redox in pH-dependent oxygen evolution on rutile ruthenium dioxide surfaces, *Chem* **2**, 668 (2017).
8. L. Bovo, C.M. Rouleau, D. Prabhakaran, and S.T. Bramwell, Layer-by-layer epitaxial thin films of the pyrochlore  $\text{Tb}_2\text{Ti}_2\text{O}_7$ , *Nanotechnology* **28**, 055708 (2016).
9. L. Fan, C.B. Jacobs, C.M. Rouleau, and G. Eres, Stabilizing Ir (001) epitaxy on yttria-stabilized zirconia using a thin Ir seed layer grown by pulsed laser deposition, *Crystal Growth & Design* **17**, 89 (2016).